Surface-atmosphere fluxes of volatile organic compounds in Beijing

W. Joe. F. Acton [1], Zhonghui Huang [2], Brian Davison [1], Will S. Drysdale [3, 4], Pingqing Fu [5],

5 Michael Hollaway [1, 6], Ben Langford [7]; James Lee [3, 4], Yanhui Liu [8, 9], Stefan Metzger [10, 11], Neil Mullinger [7.], Eiko Nemitz [7], Claire E. Reeves [8], Freya A. Squires [3]; Adam R. Vaughan [3], Xinming Wang [12], Zhaoyi Wang [12], Oliver Wild [1]; Qiang Zhang [13], Yanli Zhang [12]; C. Nicholas Hewitt [1]

10   1. Lancaster Environment Centre, Lancaster University, Lancaster, LA1 4YQ, UK
        2. State Environmental Protection Key Laboratory of Environmental Pollution Health Risk Assessment, South China Institute of Environmental Science, Ministry of Ecology and Environment, Guangzhou 510655, China
        3. Wolfson Atmospheric Chemistry Laboratories, Department of Chemistry, University of York, York,
15   YO10 5DD, UK
        4. National Centre for Atmospheric Science, University of York, York.
        5. Institute of Atmospheric Physics, Chinese Academy of Sciences, Huayanli 40, Chaoyang District, Beijing 100029, China
        6. UK Centre for Ecology & Hydrology, Library Ave, Bailrigg, Lancaster LA1 4AP, UK
20   7. UK Centre for Ecology & Hydrology, Bush Estate, Penicuik, Midlothian, EH26 0QB, UK
        8. Centre for Ocean and Atmospheric Sciences, School of Environmental Sciences, University of East Anglia, Norwich, Norfolk, NR4 7TJ, UK
        9. Peking University, 5 Yiheyuan Road, Haidian District, Beijing 100871, China
        10. National Ecological Observatory Network Program, Battelle, 1685 38th Street, Boulder, CO 80301,
25   USA
        11. Department of Atmospheric and Oceanic Sciences, University of Wisconsin - Madison, 1225 West Dayton Street, Madison, WI 53706, USA
        12. State Key Laboratory of Organic Geochemistry and Guangdong Key Laboratory of Environmental Protection and Resources Utilization, Guangzhou Institute of Geochemistry, Chinese Academy of
30   Sciences, Guangzhou 510640, China
        13. Ministry of Education Key Laboratory for Earth System Modelling, Department of Earth System Science, Tsinghua University, Beijing, China

Correspondence to: W. Joe F. Acton (w.acton@lancaster.ac.uk)

35   **Abstract.** Air pollution in Beijing has a major impact on public health and is therefore of concern to both policy makers and the general public. Volatile organic compounds (VOCs) are emitted from both anthropogenic and biogenic sources in urban environments and play an important role in atmospheric chemistry and hence atmospheric pollution through the formation of secondary organic aerosol and tropospheric ozone. Fluxes and mixing ratios of VOCs were recorded in two field campaigns as part of the Air Pollution and Human Health in a
40   Chinese Megacity (APHH) project at the Institute of Atmospheric Physics (IAP) meteorological tower in central Beijing. These measurements represent the first eddy covariance flux measurements of VOCs in Beijing giving a top down estimation of VOC emissions from a central area of the city. These were then used to validate the Multi-resolution Emission Inventory for China (MEIC). The APHH winter and summer campaigns took place in November and December 2016 and May and June 2017 respectively.

45   The largest VOC fluxes observed were of small oxygenated compounds such as methanol, ethanol + formic acid and acetaldehyde, with average emission rates of 8.02, 3.88 and 1.76 nmol m^{-2} s^{-1} respectively recorded in the summer campaign. In addition a large flux of isoprene was observed in the summer with an average flux of 4.63 nmol m^{-2} s^{-1}. While oxygenated VOCs made up 60% of the molar VOC flux measured, when fluxes were scaled by ozone formation potential and peroxyacyl nitrate (PAN) formation potential the high reactivity of isoprene and
50   monoterpenes meant that these species represented 30 and 28% of the flux contribution to ozone and PAN formation potential respectively. Comparison of measured fluxes with the emission inventory showed that the inventory failed to capture VOC emission at the local scale.

1. Introduction

55   Air quality in urban areas is a pressing issue worldwide and is becoming the subject of much scientific, political and media focus. The Chinese capital Beijing is a megacity situated on the north China plain with a population of 22 million. Beijing suffers from periods of severe air pollution resulting from pollutant emissions occurring both within the city and from sources in the wider North China Plain region (Wehner et al., 2008). This pollution has a substantial impact on human health and economic output due to the large population exposed and the commercial
60   and political importance of the city. For example, Gao et al. (2015) estimated that a single pollution event in January 2013, when the maximum hourly particulate matter (PM$_{2.5}$) concentration in Beijing reached 650 μg m^{-3}, caused 690 premature deaths and ~250 million USD in economic losses.

Volatile organic compounds (VOCs) play an important role in local and regional scale air quality through oxidation and condensation to form secondary organic aerosol (SOA) (Hallquist et al., 2009; Ehn et al., 2014) and
65   their contribution to ozone formation in the presence of NO$_x$ (Fehsenfeld et al., 1992). In addition, some VOCs, e.g. benzene, have direct detrimental impacts on humans and animals. Urban areas, especially major cities, are important sources of these compounds into the atmosphere (Langford et al., 2009; Valach et al., 2015; Karl et al., 2018) but the actual emission rates of VOCs from surface sources to the atmosphere in urban areas have, until very recently, only been estimated using inventory studies, and have not been directly measured.

70   Several studies have reported VOC concentrations in Beijing with alkanes, aromatics and oxygenated VOCs identified (Shao et al., 2009; Yuan et al., 2012; Wang et al., 2015). A positive matrix factorization (PMF) model

applied by Wang et al. (2015) identified four major sources of VOCs: two transportation factors denoted "gasoline evaporation and vehicular exhaust no. 1" and "vehicular exhaust no. 2", "natural gas and liquid petroleum gas use and background" and "paint and solvent use and industry". Biogenic VOCs (BVOCs) represent an additional

75 source of VOCs into the urban environment, the relative importance of which varies from city to city and from season to season. Ghirardo et al. (2016) used leaf-level emission measurements to estimate that BVOC emissions in Beijing, including sesquiterpenes, benzenoids and fatty acid derivatives, doubled from 2005 to 2010.

In most cities of the world it is very difficult to directly observe the effectiveness of pollution control measures on ambient concentrations in real time. However, in Beijing the strict short-term emission controls applied during

80 the 2008 Olympic Games (Liu et al., 2015) and the 2014 Asia-Pacific Economic Cooperation (APEC) summit (Li et al., 2017) allowed the impact of pollution control measures in Beijing and the surrounding area on VOC concentrations to be investigated. Liu et al. (2015) reported that the emission controls during the 2008 Olympic Games caused a concentration reduction of 13 – 20% in a range of oxygenated VOC species but that acetone concentrations remained unaffected. Li et al. (2017) found that when emission controls were applied to Beijing

85 alone only a small decrease in VOC concentrations was observed but when controls also covered surrounding cities a large decrease (>40%) in most anthropogenic VOC concentrations was observed. This indicates that the atmospheric transport of pollutants from surrounding areas makes a large contribution to VOC concentrations in Beijing.

The impact of VOC emissions on local and regional air quality is examined using atmospheric chemistry and

90 transport models, which rely on accurate estimates of the surface – atmosphere emission rates of pollutants. Much of the air quality modelling in Beijing relies on the Multi-resolution Emission Inventory for China (MEIC; available at http://www.meicmodel.org/, Qi et al. 2017) developed at Tsinghua University (e.g. Zhang et al., 2015; Hu et al., 2016). This relies on estimates of both source-specific emission factors and activity factors and is hence a "bottom-up" estimation of emissions within a defined grid square. Validation of such an inventory is important

95 in order to ensure they accurately represent real world emissions (Zhao et al. 2017). A few attempts have been made to validate VOC emissions inventories in urban areas using micrometeorological methods at the cityscape scale (e.g. Langford et al., 2009; Valach et al., 2015; Vaughan et al., 2017; Karl et al. 2018) but this has not, until now been attempted in Beijing.

In this study we present the results of two intensive measurement campaigns covering both summer and winter

100 conditions in Beijing. VOC mixing ratios were recorded using a proton transfer reaction time-of-flight mass spectrometer (PTR-ToF-MS) at a location in central Beijing. These data were then used, with three-dimensional wind velocity data, to calculate emission rates (fluxes) of VOCs, using the eddy covariance method (e.g. Müller et al., 2010) for the first time in Beijing. The calculated fluxes were then compared with the MEIC emissions inventory estimates for the measurement location. The work was carried out as part of the "Sources and Emissions

105 of Air Pollutants in Beijing" (AIRPOLL) project, itself part of the joint UK-Chinese "Air Pollution and Human Health in a Chinese Megacity" (APHH) programme, described by Shi et al. (2019).

2. Methodology

2.1. Site description

110   Measurements of VOC mixing ratios and fluxes were made during two intensive measurement campaigns (winter: 12/11/2016 - 10/12/2016; and summer: 15/05/2017 - 24/06/2017) from a 325 m high meteorological mast located on the campus of the Institute of Atmospheric Physics, Chinese Academy of Sciences (IAP) in Beijing (39°58'33"N 116°22'41"E). The campus is situated north of central Beijing between the 3rd and 4th ring roads, with

115   parkland to the east and west and a mix of dense residential and commercial (restaurants and shops) buildings to the north and south. Busy roads are situated 120 m north and 300 m east of the mast. The sample inlet for flux measurements was located at 102 m above ground level. For comparative purposes, the sampling location can therefore be described as being "urban background" in central Beijing with the main sampling inlet being significantly elevated above ground level.

2.2. Instrumental setup

120   A PTR-ToF-MS 2000 (Ionicon Analytik GmBH, Innsbruck) was housed in an air-conditioned container ~10 m from the base of the mast. This instrument principle is described in detail by Jordan et al. (2009). The PTR-ToF-MS subsampled from two inlet systems, a common flux inlet line and a gradient switching system. The common flux inlet was 0.5 inch O.D. (I.D 3/8 inch) PFA and sampled air from ~50 cm below a sonic anemometer (Gill R3,

125   Gill Instruments, Lymington, UK) which was mounted on a 3 m horizontal boom positioned on the mast at a height of 102 m above ground level. Air was drawn through the inlet line using a rotary vane pump (Model VT4.8; Becker, Hull, UK). The flow rate in the inlet line was recorded using a mass flow meter (TSI Mass Flowmeter 4043, TSI, Shoreview, USA) and remained in the range 90 - 103 L min⁻¹ during both campaigns. At 90 L min⁻¹ the Reynolds number in the inlet line is 12900, indicating turbulent flow. Particulates were removed from the air

130   flow by a 90 mm Teflon filter installed near the inlet. This filter was replaced each day.

To minimise the impact of the tower on flux measurements the sonic anemometer was positioned so that air from the prevailing wind directions would not be disturbed by the tower. In the winter the sonic anemometer was installed on the North West side of the tower and the South East in the summer. Analysis of the turbulence characteristics (Squires et al., 2020) did not show an impact from the structure even when the air flow passed

135   through the tower. This is likely due to the open lattice construction of the tower and the predominance of larger eddy scales at 102 m.

Gradient measurements were made by switching between five sampling heights (3, 15, 32, 64 and 102 m) and zero air. Air was drawn down five separate 0.25 inch O.D. (I.D. 1/8 inch) PFA lines using a common second rotary vane pump (Model VT4.8; Becker, Hull, UK). For each height the flow was sampled at 3.3 L min⁻¹ of

140   which ~300 ml min⁻¹ were drawn through a 10 L stainless steel container and an additional bypass flow of 3 L min⁻¹ was used to reduce the residence time in each line (Fig. 1). The five containers were heated to 30 °C to limit adsorption/desorption effects and had a turn-over time of approximately 30 minutes. Each hour the PTR-ToF-MS sequentially subsampled from the flow exiting each container for two minutes via a manifold valve, providing hourly 30-minute average mixing ratio at each of the five heights. The PTR-ToF-MS was operated in an hourly

145   cycle switching between the flux and gradient measurements. The PTR-ToF-MS sampled from the gradient

system for the first twenty minutes of each hour and from the flux line for the final 40 minutes of the hour. Zero air was generated using a zero air generator, built in house, made of a platinum catalyst heated to 260 °C and was sampled for 5 minutes each hour at the end of the gradient cycle.

150 The PTR-ToF-MS was operated with an inlet flow rate of 30 sccm and an E/N ratio (where E is the electric field strength; N is the buffer gas density) of 130 Td. To achieve this, the drift tube was maintained at 60 °C with a pressure 1.9 mbar and a voltage of 490 V applied across it. Data were acquired by the PTR-ToF-MS at a 5 Hz time resolution allowing VOC fluxes to be calculated using the eddy covariance method. In order to facilitate mass calibration, trichlorobenzene was introduced by diffusion through a needle valve into the inlet stream.
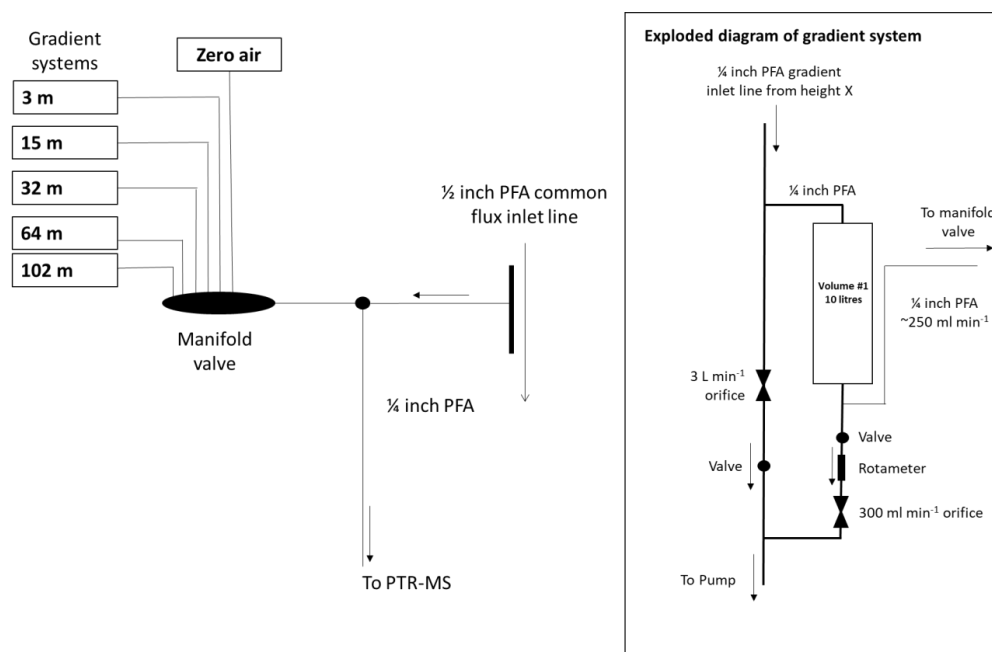
155 Figure 1: Schematic of the gradient sampling system.

2.3. Calibration

The PTR-ToF-MS was calibrated twice weekly using a 15 component VOC standard (National Physical Laboratory, Teddington, UK) during both the winter and summer campaigns. This standard contained methanol,
160 acetonitrile, ethanol, 1,3-butadiene, acetone, isoprene, butenone, butan-2-one, benzene, toluene, m-xylene and 1,2,4-trimethylbenzene at 1 ± 0.1 ppmv each. The standard was dynamically diluted in zero air to provide a six point calibration. The sensitivities to these compounds in the winter and summer campaigns are summarised in the supplementary information.

During the winter campaign, the instrument was also calibrated three times using a second independent 15
165 component VOC standard (Ionicon Analytik, Innsbruck, Austria) containing methanol, acetonitrile, acetaldehyde,

ethanol, acrolein, acetone, isoprene, crotonaldehyde, butan-2-one, benzene, toluene, o-xylene, chlorobenzene, α-pinene and 1,2-dichlorobenzene at 1 ± 0.05 ppmv each. At the end of the campaign the PTR-ToF-MS was also calibrated using an aldehyde standard (Ionicon Analytik, Innsbruck, Austria) made up of formaldehyde, acetaldehyde, acrolein, propanal, crotonaldehyde, butanal, pentanal, hexanal, heptanal and octanal at 1 ± 0.05

170   ppmv each, nonanal at 600 ± 0.07 ppb and decanal at 500 ± 0.08 ppb. Calibration using both Ionicon standards was performed following dynamic dilution in zero air to give a six point calibration. In the summer campaign four point calibrations were performed using both Ionicon VOC standards once a week.

2.4. Volume mixing ratio calculation

PTR-ToF-MS mass calibration and peak fitting was performed on the 5 Hz data using PTRMS Viewer 3 (Ionicon

175   Analytik, Innsbruck). VOC mixing ratios were then calculated using the method based on that previously applied by Acton et al. (2016), Tani et al. (2004) and Taipale et al. (2010). Counts per second (cps) of each protonated VOC species (RH^+) were normalized against the primary ions (H_3O^+ and the $H_2O.H_3O^+$ cluster ion) and background counts were subtracted to give background corrected normalised count rates $I(RH^+)_{norm}$:

180
$$I(RH^+)_{norm} = I(RH^+) \left(\frac{I_{norm}}{I(H_3O^+) + I(H_3O^+H_2O)} \right)$$
(1)

$$- \frac{1}{n} \sum_{i=1}^{n} I(RH^+)_{zero,i} \left(\frac{I_{norm}}{I(H_3O^+)_{zero,i} + I(H_3O^+H_2O)_{zero,i}} \right),$$

where $I(H_3O^+)$ and $I(H_3O^+H_2O)$ represent the measured count rate for H_3O^+ and the $H_3O^+H_2O$ cluster, respectively. Zero air measurements were labelled using the subscript zero and the number of zero air

185   measurements was represented by n. The total reagent ion count rate (H_3O^+ and $H_3O^+H_2O$) was normalised to a count rate of 10^6 cps (I_{norm}).

Following calculation of the background corrected normalised count rate, the volume mixing ratio (VMR) was calculated, as a wet mass fraction, as:

$$VMR_{VOC} = \frac{I(RH^+)_{norm}}{S_{norm}} \qquad ,$$
(2)

190   where S_{norm} is the normalised sensitivity (ncps/ppb) for each mass calculated using a transmission curve as described by Taipale et al. (2008). Mixing ratios of specific compounds were then determined by summing parent ion and fragment ion mixing ratios. For direct comparison with the molar flux the volume mixing ratio was converted to a molar concentration (χ_{VOC}) using equation 3.

$$\chi_{VOC} = \frac{P \times VMR_{VOC}}{R \times T},$$
(3)

195   where P is the atmospheric pressure, T is atmospheric temperature and R is the molar gas constant (8.314 J K^{-1} mol^{-1}).

2.5. Flux calculation

The continuous fast measurement of PTR-ToF-MS for all compounds allows the estimation of fluxes using direct eddy covariance rather than the virtual disjunct eddy covariance methods that had to be applied when using older

200 PTR-quad-MS instruments (e.g. Karl et al., 2002; Langford et al., 2009). Eddy-covariance fluxes of VOCs using PTR-ToF-MS were first made by Müller et al. (2010). A detailed description of flux estimation using eddy covariance is provided by Aubinet et al. (2012). Here fluxes were calculated using the eddy4R routines (Metzger et al., 2017). The flux (F_x) of each compound was determined by calculating the covariance function between the vertical wind velocity (w) and the VOC mixing ratio (VMR_x):

205 $$F_x(\Delta t) = \frac{1}{N} \sum_{i=1}^{N} w'(i - \Delta t/\Delta t_w) VMR_x'(i), \tag{4}$$

where w' and VMR' represent momentary deviations from the mean volume mixing ratio or vertical wind speed (i.e. $w' = w - \bar{w}$). N is the number of PTR-ToF-MS measurements in our half hour averaging window (9000 for 5 Hz measurements), Δt_w is the sampling interval between wind measurements (0.2 s) and Δt is the lag time between the vertical wind measurements recorded by the sonic anemometer at 102 m and the mixing ratios

210 recorded using the PTR-ToF-MS instrument at ground level.

The lag time between the vertical wind velocity measurement and VOC mixing ratio measurement is primarily controlled by the inlet line length and the flow rate in the line. However, small variations in temperature, pressure, humidity and pump performance, and also horizontal displacement between anemometer and inlet coupled with changes in wind speed and direction can all cause deviation in the lag time. The lag time can be determined by

215 assessing the covariance between w and VMR as a function of time. The lag time can then be identified by selecting the maximum of this covariance function (Taipale et al., 2010). For many of compounds recorded in this study only a weak flux was observed. This results in a low signal-to-noise ratio, introducing a large uncertainty into the identification of the cross-covariance maximum. Adsorption and desorption rates to the inlet line are compound specific and dependent on polarity. Therefore, the lag times for more polar compounds such as oxygenated VOCs

220 will differ slightly from pure hydrocarbons, however, weak covariance peaks made the identification of the lag-times difficult for many masses. Lag times were therefore determined by calculating the lag for compounds where a strong covariance peak was observed (isoprene and C2-benzene (C_8H_{10}) in the summer and winter campaigns respectively) and applying their modal lag times as a fixed value to all masses. The calculation of lag time for eddy-covariance data with low signal-to-noise ratio is described in detail by Langford et al. (2015).

225 The effect of storage below the measurement height was calculated for flux averaging period t as:

$$Storage\ F_{x\,t} = h\frac{\chi_{x\,t-1} - \chi_{x\,t+1}}{3600} \quad . \tag{5}$$

Where $\chi_{x\,t-1}$ and $\chi_{x\,t+1}$ are the concentration (nmol m^{-3}) of compound X in the averaging periods before and after flux averaging period t and h represents the measurement height in meters (102 m). This method was chosen so as to be comparable with the other flux measurements made during this project (e.g. Squires et al. 2020). This

230 storage term was then added to the calculated turbulent flux term. At the 102 m measurement height large eddies mean that some of the flux may not be captured in the 30 min flux averaging period used here. This loss of low frequency flux was investigated by Squires et al. (2020) who found that at the 102 m measurement height the flux

loss was ca. 7%. Loss of high frequency flux was due to measuring at 5 Hz was estimated to be less than 10%. Squires et al. (2020) estimated that the average the time taken for an air parcel to reach the inlet point at 102 m

235 was ~68 s, assuming a OH concentration of 1×10^6 molecules cm^{-3} and an ozone concentration of 1.2×10^{12} molecules cm^{-3} ~1% of monoterpenes (the most reactive species recorded) would have reacted before the measurement height.

Half hour averages were quality assessed using three tests after a 2-dimensional coordinate rotation to correct for tilting of the sonic anemometer. The limit of detection was calculated for each mass by determining the cross-

240 covariance between 150-180 s, a region outside the expected time lag range (Spirig et al., 2005). The stability of the flux across the half hour averaging period was assessed using the method described by Foken and Wichura (1996). Flux files were filtered where the stationarity criterion exceeded 60% and were above the limit of detection. This was because for fluxes below the limit of detection a robust statement on their stationarity could not be made. Lastly, files were also flagged if the mean frictional velocity (u_*) fell below 0.175 m s^{-1}. This

245 threshold was derived from assessment of the u* dependence of the sensible heat flux. Data falling below this threshold were substituted by the campaign average value for that hour so as not to introduce a positive bias to the VOC flux. The random error of each half hour flux average was assessed using the method described by Lenschow et al. (1994) and fluxes with a relative random error greater than 150%, averaged across the campaign, were discarded.

250

3. Results and Discussion

3.1 Meteorology
The main APHH-Beijing winter measurement campaign ran from the 7th November - 10th December 2016 (Shi et

255 al., 2019) with the PTR-ToF-MS operating from 22nd November - 12th December 2016. During this period, wind speeds were low, ranging between 0.3 and 9.7 m s^{-1}, with a mean value of 2.4 m s^{-1}, and with the highest wind speeds observed from the North West (Fig. 2). The predominant wind directions were southerly and north westerly. Temperatures, measured at 102 m on the IAP meteorological tower, ranged from -7 to 15 °C with a mean value of 3.6 °C. Relative humidity ranged from 15 to 92% with a mean value of 45% (Fig. 3). Precipitation

260 was small during the campaign period with light rain on 20th November and snow on 21st November.
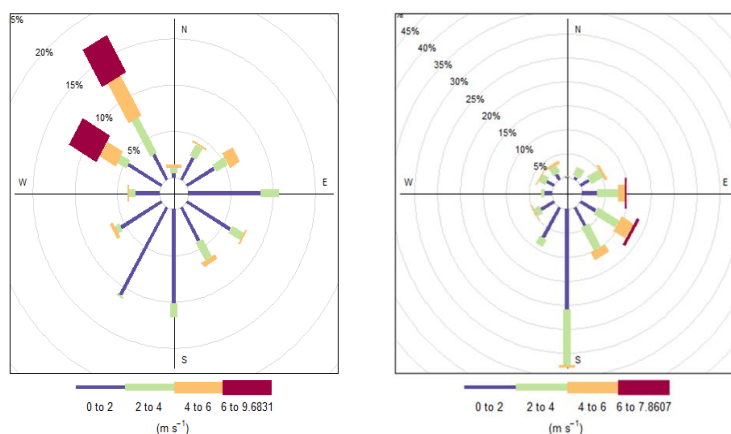
Figure 2: Wind conditions during the winter campaign (left) and summer campaign (right). The plots show the percentage of time the wind was from each direction and are coloured by wind speed.

The principal APHH-Beijing summer measurement campaign ran from 20th May - 22nd June 2017 (Shi et al., 2019) with the PTR-ToF-MS operational from 21st May - 25th June 2017. Wind speed during this campaign ranged between 0.5 and 7.9 m s^{-1}, with a mean value of 2.3 m s^{-1}. The predominant wind direction was south-easterly (Fig. 2). Temperatures at 102 m ranged from 15 to 37 °C with a mean value of 25 °C and the relative humidity ranged from 13 to 93% with a mean value of 44% (Fig. 3). Precipitation was low during the campaign period with light rain observed on 22nd and 30th May and on 2nd, 6th, 18th and 21st – 23rd June.
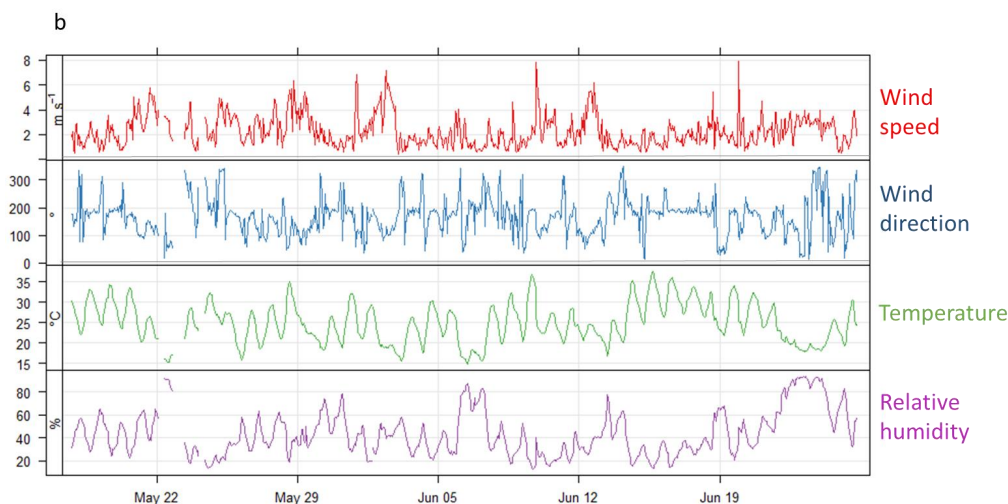
Atmospheric
Chemistry
and Physics
Discussions
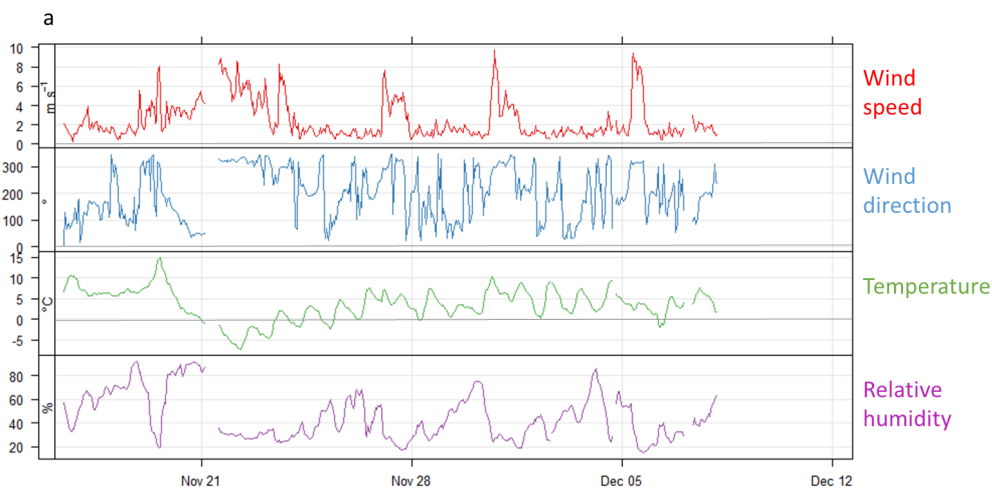
Figure 3: Summery of meteorological data in winter measurement campaign (a) and summer measurement campaign (b).

275

3.2 Flux footprint

The flux footprint was calculated for each half hour flux averaging period of both field campaigns using the method described by Kljun et al. (2004) and Metzger et al. (2012). The calculation of the flux footprint for this campaign is described in detail by Squires et al. (2020). During both the summer and winter field campaigns 90%

280 of the measured flux originated from an area within 7 km of the IAP meteorological tower, however, 90% of the contribution to the campaign average flux footprint extended just 2 km from the tower. Mean flux footprint climatologies for the summer and winter campaigns are displayed in Fig. 4, with contour lines showing the distances from the tower where the surface contributions to the measured fluxes cumulate to 30, 60 and 90%, respectively. In the winter campaign the main contribution to the average flux was predominantly from the North

285 West and South East, encompassing two large roads: the Jingzang Expressway and the Beitucheng West Road and a mix of commercial and residential buildings, and urban park land. In the summer campaign the largest contribution to the flux came from regions approximately 1 km south west of the tower and approximately 1 km north east of the tower now encompassing different sections of the Jingzang Expressway, Beitucheng West Road, residential buildings, commercial buildings (shops and restaurants) and a larger contribution from urban park land

290 compared to the winter campaign.

Figure 4. The campaign mean flux footprint climatologies for the winter (left) and summer (right) field campaigns. The IAP meteorological tower is represented by the red dot and surrounding 100 x 100 m cells are coloured by their mean contribution to the flux. The contour lines correspond to the distances from the tower

295   where the surface contributions to the measured fluxes cumulate to 30, 60 and 90% respectively. Map tile sets are © Stamen Design, under a Creative Commons Attribution (CC BY 3.0) license.

3.3. VOC mixing ratios

In the winter campaign the detected VOC species with the largest mixing ratios were the small oxygenated VOCs

300   (OVOCs) methanol, acetaldehyde and acetone, with median mixing ratios of 19.29, 4.59 and 2.57 ppb, respectively. Large mixing ratios of aromatic compounds were also observed, with median mixing ratios between 1.5 and 2.0 ppb for each of benzene, toluene and C_2-benzenes. Mixing ratios of these compounds tracked the pollution events in a distinctive "sawtooth cycle" described by Jia et al. (2008). Mixing ratios increased over a period of 3 - 4 days when the wind speed was low and prevailing wind direction was southerly before dropping

305   rapidly when the wind direction moved to the North West. In the summer campaign the dominant VOC species observed were again methanol, acetaldehyde and acetone (26.39, 3.50 and 3.67 ppb respectively), but the mixing ratios of aromatic compounds were lower, with median values of 0.30, 0.37 and 0.47 ppb observed for benzene, toluene and C_2-benzenes respectively. In addition, isoprene, which has both biogenic and anthropogenic sources, had a median mixing ratios of 1.08 and 0.38 ppb in the winter and summer campaigns respectively. In contrast to

310   the winter campaign, VOC mixing ratios during the summer campaign showed a clear diurnal cycle with mixing ratios peaking at night and dropping during the day as the planetary boundary layer expanded during the day-time and contracted at night-time. A summary of VOC mixing ratios for the principal VOC species observed during the two campaigns are displayed in Table 1. For a more detailed discussion of VOC mixing ratios recorded during this campaign see Zhang et al. (2019).

315

Table 1. Summary of VOC mixing ratio for the dominant VOCs observed in Beijing during APHH-Beijing winter and summer campaigns (in ppb).

	Methanol	Acetonitrile	Acetaldehyde	Acetone	Isoprene	Benzene	Toluene	C_2-Benzenes
Winter campaign								
Max	93.98	2.13	17.42	9.66	4.50	9.11	9.43	13.07
Min	0.00	0.00	0.22	0.00	0.00	0.00	0.00	0.00
Median	19.29	0.38	4.59	2.57	1.08	1.59	1.65	1.65
Mean	24.32	0.51	4.92	2.80	1.21	2.00	1.94	2.08
Standard deviation	20.83	0.51	3.66	2.00	1.03	1.74	1.87	2.07
Summer campaign								
Max	73.75	24.44	26.92	11.76	3.24	1.89	2.74	3.41
Min	7.10	0.00	0.00	0.70	0.00	0.00	0.00	0.00
Median	26.39	0.29	3.50	3.67	0.38	0.30	0.37	0.47
Mean	28.39	0.97	4.64	3.86	0.56	0.37	0.46	0.60
Standard deviation	11.02	1.86	3.57	0.44	0.55	0.31	0.37	0.52

320

3.4 VOC fluxes

The mixing ratio values represent the ambient concentrations observed at the sample inlet averaged over the sampling period. However, by combining these mixing ratios with the three dimensional wind vector, the eddy covariance flux calculation method allowed for quantification of the net exchange (flux) of the observed
325   compounds from a surface "footprint". The size of this footprint depends on the height of measurement, surface roughness and a number of meteorological factors, including wind speed and atmospheric stability. Under the conditions pertaining in Beijing, 90% of the campaign average measured flux originated from an area within 1-2 km of the tower. The fluxes observed at 102 m are therefore predominantly controlled by local emissions, unlike the mixing ratios observed at the same point which are influenced by both local and more distant emissions,
330   chemical processing and meteorology.

Greater surface solar heating in the summer led to increased turbulence than in the winter, with median u_* values of 0.41 and 0.26 m s^{-1} respectively. This meant turbulent transport was more easily measured, allowing the fluxes of a larger number of compounds to be quantified than in winter. Of the 179 masses observed in the summer campaign for which sufficient data was obtained to allow quantification, 65 masses gave a flux with a median
335   relative random error of less than 150%. These masses all showed a net positive flux with no masses showing net deposition. Molecular formula were assigned to 50 of these masses using their exact mass, while 15 masses with a small negative mass defect could not be allocated a formula, based on the combination of C, H, N, O, S and Cl

within 0.1 mDa of the recorded mass. Mass spectral peaks observed at m/z 47.019 and 47.053, assigned to formic acid and ethanol, respectively, could not be sufficiently resolved so these compounds were considered together.

340   Diurnal cycles of the six compounds with the largest fluxes are shown in Fig. 5 (solid lines), showing the large VOC flux observed in the summer campaign in comparison to the much smaller fluxes observed in the winter campaign. This figure also displays fluxes without the storage term applied (dashed lines) and the gap-filled u_* filtered flux (dotted lines). As shown, these corrections have only a small impact on the fluxes calculated. The fluxes of these six compounds are summarised in Table 2. As shown in Table 2 fluxes of all compounds were

345   larger in the summer than in the winter. This was not the case for NO_x and CO which were larger in the winter than in the summer (Squires et al., 2020). The weak VOC flux observed in the winter may, in part, be caused by low volatilisation of VOCs in winter conditions, where the average temperature was 3.6 °C compared to 25 °C in the summer. In the winter the positive (emission) flux of VOCs from the city is likely suppressed by deposition of VOCs transported at, high concentrations, from outside of the city. While most mean winter VOC fluxes

350   remained positive this term will be a balance between emission from the city and deposition of VOCs transported into the footprint region. As the low winter fluxes were difficult to accurately quantify our analysis focuses on the fluxes recorded during the summer campaign.

355

360

365

Table 2: Summary of (storage corrected) fluxes of VOCs displayed in Table 1 including the six dominant VOC fluxes recorded in Beijing during APHH-Beijing winter and summer campaigns (in nmol m^{-2} s^{-1}).

	Methanol	Acetonitrile	Acetaldehyde	Formic acid + Ethanol	Butene	Acetone	Acetic acid	Isoprene	Benzene	Toluene	C$_2$-Benzene
					Winter campaign						
Max	56.37	1.22	11.45	8.45	2.58	3.87	11.24	24.42	4.49	3.70	4.60
Min	-48.63	-0.71	-7.21	-8.35	-1.77	-2.24	-8.71	-8.17	-2.93	-2.64	-2.81
Median	1.58	0.08	0.40	0.37	0.09	0.02	0.43	0.51	0.11	0.19	0.19
Mean	2.15	0.11	0.54	0.57	0.12	0.12	0.44	0.79	0.17	0.23	0.26
Standard deviation	9.92	0.24	1.89	1.92	0.49	0.68	2.37	2.34	0.72	0.64	0.80
					Summer campaign						
Max	55.36	10.64	11.89	53.67	16.42	7.65	14.24	45.83	2.78	18.16	12.76
Min	-21.33	-17.63	-3.57	-4.19	-1.23	-1.81	-3.20	-1.92	-1.05	-0.76	-0.80
Median	6.21	0.15	1.41	2.98	1.07	0.74	1.22	2.00	0.25	0.54	0.55
Mean	8.02	0.17	1.76	3.88	1.57	0.94	1.56	4.63	0.31	0.85	0.83
Standard deviation	7.79	1.08	1.79	4.57	1.86	0.96	1.85	6.60	0.29	1.37	1.20

370

3.4.1 Total measured VOC flux

In the summer campaign the total measured VOC flux was strongly positive with the city centre acting as a net source of VOCs into the atmosphere. In the winter campaign there was a small net positive flux of most identified VOC species but at some times deposition of VOCs was also observed (Fig. 5). The total measured VOC fluxes

375 and concentrations during the summer field campaign, coloured by compound class, are displayed in Figs. 6a and 6b respectively, with the total measured VOC flux peaking at 90 nmol m^{-2} s^{-1} at mid-day. As alkanes have a proton affinity less than that of water these compounds can't be measured using PTR-MS so are not included here.

Of the compounds measurable by PTR-MS, oxygenated compounds have the largest sum mixing ratio observed above Beijing. Methanol and ethanol + formic acid together account for approximately one third of the total

380 oxygenated VOC mixing ratio. These compounds have been observed at high concentrations in many cities (Langford et al., 2009; Valach et al. 2014) with ethanol reported to be the most abundant VOC in London (Dunmore et al., 2016). Methanol and ethanol + formic acid together also make up one third of the total molar flux. Other oxygenated compounds together make up another 31% of the summer flux. This is consistent with the

large flux of oxygenated VOCs observed by Karl et al. (2018) from the urban canopy in Innsbruck, Austria.

385   Unclassified compounds made up primarily of masses corresponding to compounds containing nitrogen, sulphur and halogens make up 15% of the total concentration, but these masses contribute only 9% to the total flux. The (non-oxygenated) hydrocarbons have been divided into three categories: biogenic compounds (isoprene and monoterpenes), aromatic compounds and other hydrocarbons. Together these compounds make up 15% of the total VOC mixing ratio observed but make up 31% of the total measured VOC flux, with biogenic compounds the

390   largest contributors.
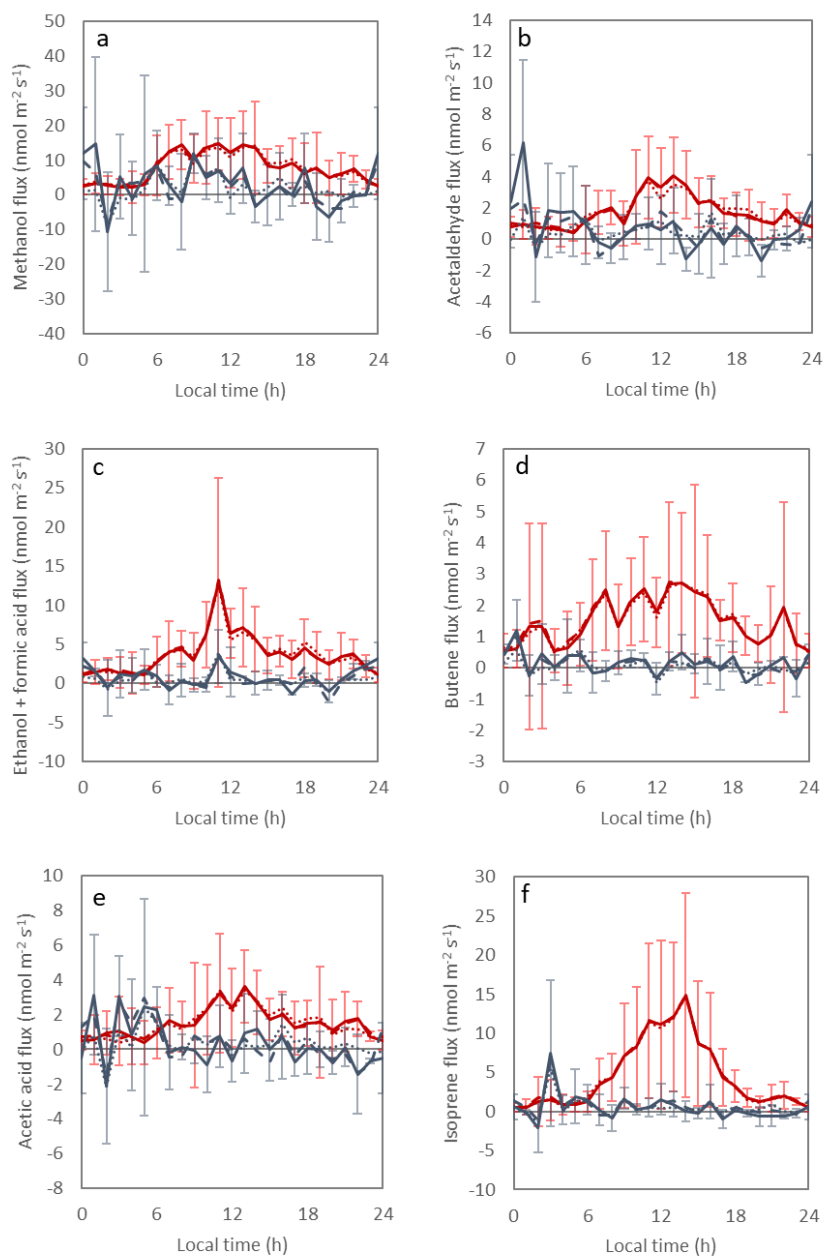
Figure 5: Diurnal cycles of the fluxes of six compounds with the largest observed fluxes for the summer (red) and winter (blue) campaigns, with error bars showing standard deviation of the stationarity filtered and fluxes including the storage term (solid lines). Dashed lines represent the flux without the storage term and dotted lines are u_* filtered fluxes including the storage term and gap filled with the average flux above the u_* threshold for that hour.

395

3.4.2 Anthropogenic VOC fluxes

Combustion products are a major source of anthropogenic VOCs in urban areas. The relationship between the fluxes of VOC species which contribute more than 0.75% to the total measured VOC flux and the NO_x flux in the summer measurement period is shown in Fig. 7. NO_x fluxes during the campaigns have previously been reported by Squires et al. (2020). NO_x in urban areas is a combustion product so the NO_x flux is used here as proxy for combustion sources of pollutants. The fluxes of the aromatic VOCs toluene, C_2-benzenes (the sum of xylenes and ethyl benzene which cannot be separated using PTR-MS) and C_3-benzenes (the sum of all compounds featuring a benzene ring and three methyl groups) show a good correlation with the fluxes of NO_x, with R^2 values of 0.75, 0.64 and 0.61, respectively. Fluxes of toluene, C_2 and C_3 benzenes all follow a similar diurnal profile, after a small peak in the early morning emissions increase from 06:00 and peak between 10:00 and 15:00 and then decrease in the evening with another small peak at 22:00. As shown in Fig. 7 the fluxes of aromatic compounds were closely correlated suggesting that they are emitted from the same source. Beijing operates an emissions control program which only allows non-local heavy duty vehicles to enter the city between 00:00 and 6:00 (Yang et al., 2015) and this may explain the peak in aromatic emission observed at 02:00 (Fig. 6). These compounds are known to be combustion products and are also emitted by evaporation. These fluxes are discussed in detail by Squires et al. (2020) who found that while the winter benzene and toluene fluxes (0.01 and 0.03 nmol m^{-2} s^{-1}, respectively) were smaller than those observed in London and Manchester, the Beijing summer fluxes (0.18 and 0.61 nmol m^{-2} s^{-1} for benzene and toluene, respectively) were comparable to those reported in the UK (Langford et al., 2009; Langford et al., 2010; Valach et al., 2015; Vaughan et al., 2017). Squires et al. (2020) also concluded that the benzene/toluene ratio, which for concentrations was 0.89 in the winter and 0.73 in the summer, and for fluxes 0.72 in winter and 0.31 in summer, was within the range expected for primary exhaust emissions.

The fluxes of other compounds shown to correlate with the flux of NO_x were propene and methanol with R^2 values of 0.63 and 0.71. Propene emissions are likely driven by the evaporation of petrochemicals and have previously been recorded in plumes of VOCs released from industrial activity (Karl et al., 2003). Large fluxes of propene were recorded, with average emissions of 0.64 and 0.93 nmol m^{-2} s^{-1} in the winter and summer, respectively. In the winter the strongest emission occurred early in the morning with little emission later in the day. In the summer measurement period, emissions increased from 06:00 before peaking at mid-day and decreasing in the late afternoon. Methanol is emitted from plants and industry and is formed by oxidation reactions in the atmosphere (Jacob et al., 2005). It is also present in many consumer goods products (Steinemann, 2015). The close correlation with the NO_x flux and aromatics such as toluene suggests a combustion source contributes to the total methanol flux but the summer methanol flux also correlates well with small oxygenated VOCs such as acetaldehyde. Methanol had the largest molar flux of any VOC species recorded in the summer (Fig. 5), with average emissions of 2.15 and 8.02 nmol m^{-2} s^{-1} in the winter and summer, respectively. These methanol emissions are comparable to those observed in London with 2.5 nmol m^{-2} s^{-1} (August to December) recorded by Valach et al. (2015) and 8.2 nmol m^{-2} s^{-1} (October) reported by Langford et al. (2010). Methanol mixing ratios were, however, significantly higher in Beijing than in London with average mixing ratios in Beijing 28.2 and 24.3 ppb in the winter and summer compared with 7.5 and 19.4 ppb reported by Valach et al. (2015) and Langford et al. (2010) at 61 and 200 m, respectively.

Acetonitrile is considered a tracer for biomass burning (de Gouw et al., 2003), but can also be produced by the burning of fossil fuels (Holzinger et al., 2001). Acetonitrile fluxes in the summer field campaign were low with a median value of 0.15 nmol m^{-2} s^{-1} but regularly peaked between 16:00 and 18:00 in the evening with a maximum value of 10.6 nmol m^{-2} s^{-1}, so potentially indicating a cooking source. In the winter the median acetonitrile flux

440   was small (0.11 nmol m^{-2} s^{-1}) with peaks of up to 1.21 nmol m^{-2} s^{-1} observed in the early hours of the morning. As cooking rates are likely to be comparable in the summer and winter the reduced winter acetonitrile flux could be explained by reduced ventilation of homes in the winter.
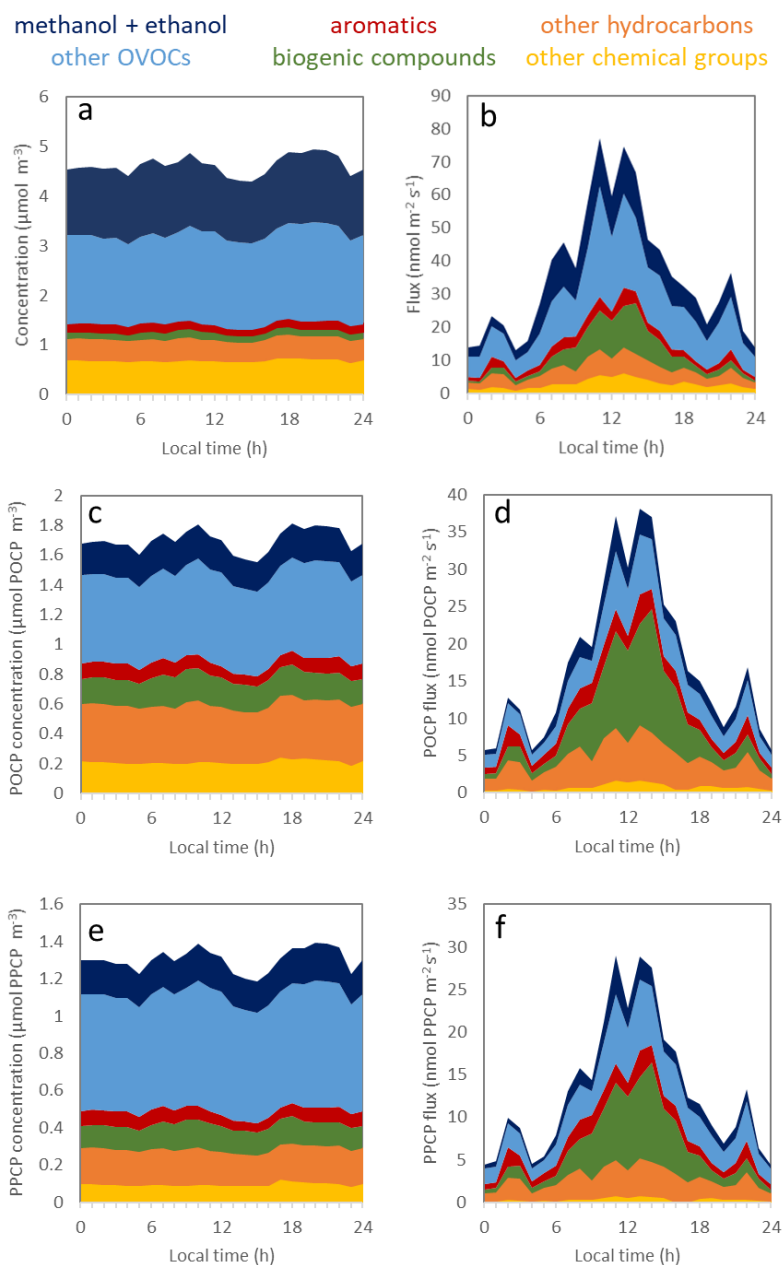
Figure 6. Total observed VOC concentration (a) and flux (b) measured during the summer field campaign,
445   scaled using POCP (c, d) and PPCP (e, f).
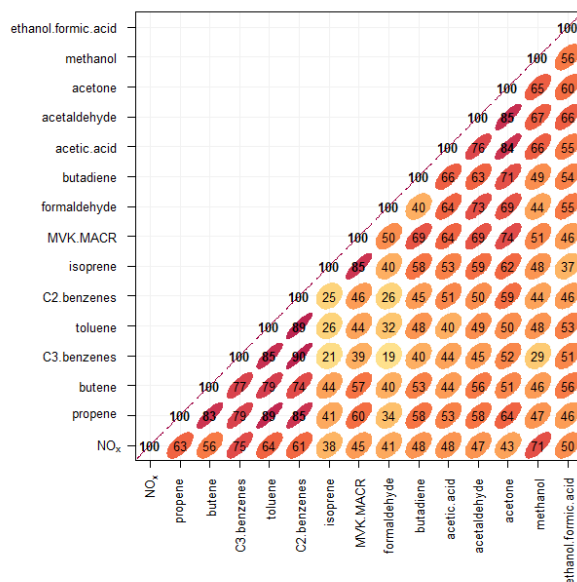
Figure 7. Correlation plot showing the relationship between the fluxes of all identified compounds that contribute more than 0.75% to the total measured VOC flux in the summer measurement campaign as well as the NO_X flux. Numbers and colour represent the % R^2 value of each correlation.

450

3.4.3 Biogenic fluxes

Globally, plants are the main source of VOCs into the atmosphere, with isoprene and monoterpenes the main VOC species emitted (Guenther et al., 1995; 2012). Plants have also been shown to be a significant source of VOCs in urban environments with Langford et al. (2010) and Valach et al. (2015) both attributing measured

455   isoprene fluxes and concentrations in London, in part to biogenic sources. In Beijing, Ghirardo et al. (2016) used leaf level measurements to assess the impact of stress-induced BVOCs. They concluded that these stress-induced compounds were comparable to constitutive BVOC emissions in terms of their impact on SOA formation. In the current study, significant BVOC emissions were observed in the summer campaign, with average emissions of 4.63 nmol m^{-2} s^{-1} for isoprene and 0.15 nmol m^{-2} s^{-1} for monoterpenes. At night-time, emissions of both

460   monoterpenes and isoprene were close to zero with mixing ratios dropping to 0.3 ppb from a mid-day peak of 0.7 ppb. Emissions began to increase at 06:00 before peaking at mid-day and returning to zero at around 20:00 (isoprene emissions are displayed in Fig. 5). The summer isoprene flux correlated well (R^2 0.85) with the flux of the isoprene oxidation products methyl vinyl ketone and methacrolein (MVK+MACR) (Fig. 7). In the winter campaign, emissions of both isoprene and monoterpenes were comparatively small with average fluxes of 0.79

465   and 0.06 nmol m^{-2} s^{-1}, respectively. Despite the weak isoprene flux, mixing ratios were larger in winter than in summer with mixing ratios consistent through the day with an average value of 1.21 ppb. The high isoprene mixing ratio in the winter suggests transport of anthropogenic isoprene from outside of the flux footprint together

with a lower rate of photochemical loss than in the summer. The low winter isoprene flux suggested a small contribution of anthropogenic isoprene to the total flux. Sesquiterpenes were also recorded in the summer with a

470   mean mixing ratio of 0.04 ppb but a flux was not detected. The summer isoprene flux is larger than that recorded in London (Valach et al., 2015) where an average emission of 0.53 nmol m^{-2} s^{-1} was observed between August and December. This is likely due to the London emissions being reduced by the generally lower temperatures and radiation levels, due to the difference in latitude and also the inclusion of autumn and winter flux data. In the summer campaign biogenic compounds accounted for 13% of the total molar VOC flux and 42% of non-

475   oxygenated hydrocarbon emission.

Isoprene emission from biogenic sources is commonly modelled using the Model of Emissions of Gases and Aerosols from Nature (MEGAN, Guenther et al., 2006). Emission of isoprene in MEGAN is calculated as:

$$Emission \ = \ \varepsilon \ \times \ \gamma \ \times \ \rho, \tag{6}$$

where ε is an emission factor (nmol m^{-2} s^{-1}) representative of the isoprene emission from a plant canopy under

480   standard conditions, γ is a dimensionless emission activity factor representing deviation from standard conditions and ρ is a factor (normalised ratio) accounting for loss within the canopy. By default the emission factor used by MEGAN for Beijing is 11.04 nmol m^{-2} s^{-1}. The expected isoprene flux from Beijing was modelled using MEGAN together with photosynthetic photon flux density (PPFD) and atmospheric temperature recorded at the IAP metrological tower. The leaf area index (LAI) for Beijing was 1.0 for May and 1.7 in June with these values taken

485   from the MERRA-2 reanalysis data set for 2017. The flux predicted by MEGAN over-estimated the observed flux with the modelled mean diurnal isoprene flux peaking at 21 nmol m^{-2} s^{-1} compared to the measured isoprene flux which peaked at 14 nmol m^{-2} s^{-1} (Fig. 8b).

The measured isoprene flux together with the product of the emission activity factor and loss factor ($\gamma \times \rho$) can be used to optimise the emission factor (ε) for the flux footprint. Langford et al. (2017) used a weighted mean to

490   determine the isoprene emission factor which ensures that the modelled isoprene emission has the same average as the measured flux. This approach gives an emission factor of 10.16 nmol m^{-2} s^{-1} for the summer campaign. Using this emission factor MEGAN estimates a diurnal flux peaking at 18 nmol m^{-2} s^{-1}. This value is elevated by the low, anthropogenic, night time flux observed in Beijing. Alternatively an optimised isoprene emission factor can be calculated using the least-square regression between the measured isoprene flux and ($\gamma \times \rho$) (Fig. 8a). This

495   gave an isoprene emission factor of 7.57 nmol m^{-2} s^{-1}, representing an optimised emission factor for central Beijing. When using this emission factor the mean diurnal isoprene flux predicted by MEGAN peaked at 14 nmol m^{-2} s^{-1} (Fig. 8b). This compares well with the measured isoprene flux and represents a more appropriate emission factor than that calculated using the weighted mean approach. This optimised emission factor is 69% of the default MEGAN emission factor value for Beijing.
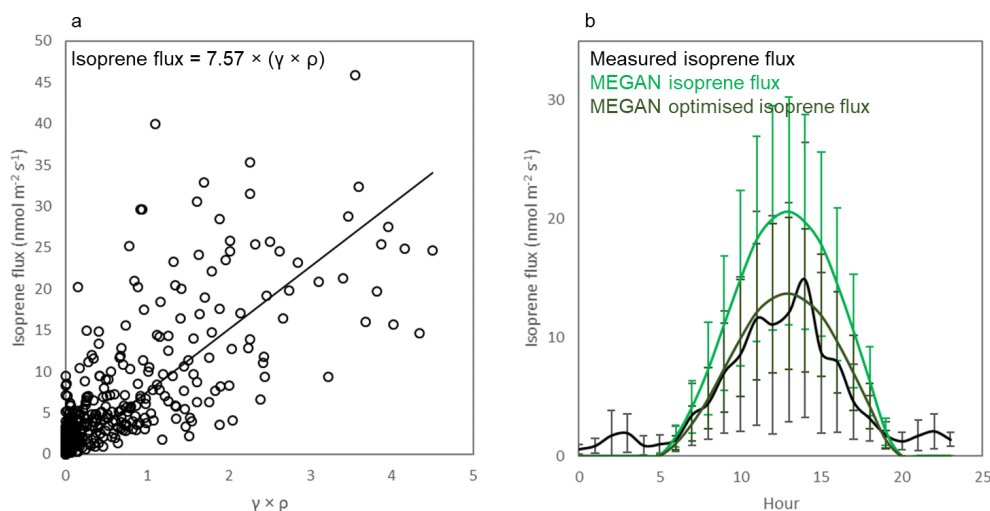
Figure 8. (a) measured isoprene flux plotted against the product of the emission activity factor (γ), and the canopy loss and production factor (ρ). (b) diurnal profiles of the isoprene flux predicted by MEGAN using the default and optimised emission factors together with the measured isoprene flux. Error bars represent standard deviation across the measurement period.

### 3.4.4 Impact on atmospheric chemistry

The relative impact of individual VOCs on ozone and peroxyacyl nitrates (PAN) formation can be determined by considering the photochemical ozone creation potentials (POCPs) and the photochemical PAN creation potentials (PPCPs) of the observed compounds. The POCP represents the increment in ground-level ozone production due to the photochemistry of that compound relative to the ozone increment due to ethane. PPCP represents the PAN increment due to the photochemistry of that compound relative to that of propene. The POCPs and PPCPs of 120 organic compounds were reported by Derwent et al. (1998) for UK conditions of the 1990s, and in the absence of more Beijing-specific data these were used to scale both the mixing ratios and the fluxes emitted within the flux footprint of the individual observed VOCs. Where a measured mass was not reported by Derwent et al. (1998) the average POCP and PPCP for the appropriate chemical class were applied. It should be noted that as alkanes cannot be detected using PTR-MS these compounds are not included here. However, due to their low POCP and PPCP relative to alkenes and many oxygenated compounds they are likely to have a relatively small impact on ozone and PAN formation.

Figures 6c and 6d show the concentrations and fluxes scaled by POCP, respectively. Of those compounds resolved by PTR-MS, biogenic compounds were the largest source of POCP making up 34% of the total POCP-scaled flux. Oxygenated compounds were also a significant source of POCP due to the large molar flux of these compounds, with methanol and ethanol + formic acid making up 13% of the POCP-scaled flux and other oxygenated VOCs 18%. The PPCP-scaled fluxes and concentrations are shown in Figs. 6e and 6f respectively and show that, as with

22

the POCP, oxygenated and biogenic VOCs are likely to make the largest contribution to photochemical PAN

525 formation.

The influence of VOCs on OH and Ozone reactivity was determined by the VOC reaction rate with the OH radical and ozone, relative to that of ethane. VOC reaction rates with the OH radical and ozone were taken from Atkinson and Arey (2003) and references therein. Biogenic compounds dominate the OH reactivity scaled VOC flux making up 51% of the potential OH reactivity emitted (Fig. 9b). Oxygenated VOCs and non-aromatic hydrocarbons

530 (predominantly butene and propene) represent 22% and 17% of the VOC flux scaled by OH reactivity respectively. The VOC concentrations scaled by OH reactivity (Fig. 9a) shows that of the VOCs measured using PTR-ToF-MS oxygenated compounds have the largest impact on OH reactivity. This is caused by the very high mixing ratios of these compounds relative to other chemical groups in the atmosphere. However once scaled by OH reactivity, biogenic compounds, which only make up 4% of the total measured VOC concentration (Fig. 9a),

535 are shown to contribute 21% to the total measured VOCs scaled by OH. Ozone reactivity is dominated by alkenes with biogenic compounds and non-aromatic hydrocarbons (predominantly butane, C_6H_{10} and C_7H_{12}) making up 31 and 61% of the potential ozone reactivity emitted respectively (Fig. 9d).
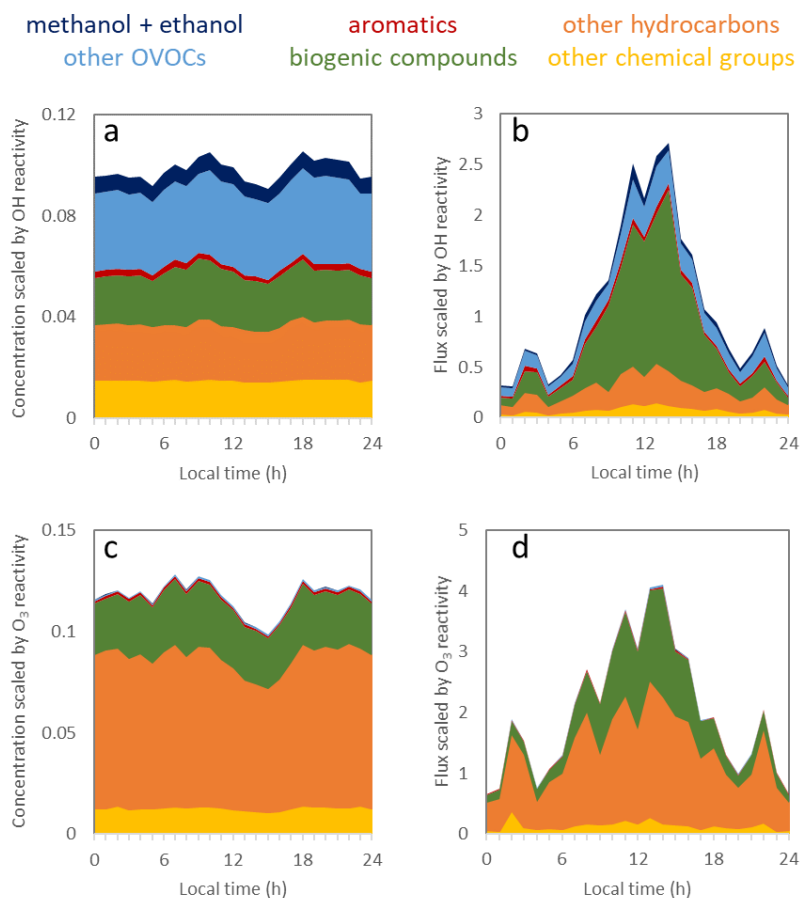
Figure 9. Total observed VOC concentration and flux measured during the summer field campaign scaled using by OH (a, b) and O_3 (c, d) reactivity relative to ethane.

3.5 Emission factor

The Multi-resolution Emissions Inventory for China (MEIC, Qi et al. 2017; http://www.meicmodel.org/) is a comprehensive inventory of the emission of atmospheric pollutants across China and provides the emissions input to many modelling studies (e.g. Hu et al. 2016). Inventories such as MEIC use emissions estimates from individual sources scaled by activity data to provide a "bottom-up" emissions estimate. Whilst activity data is often relatively well constrained at national level, its spatial disaggregation often relying on simplified proxies such as population density, adds significant additional uncertainty for the estimate of the emission for a given location. The VOC flux measurements presented here provide a "top-down" measurement at the cityscape-scale which can be used to validate the emissions inventory encompassed by the flux footprint. Zhao et al. (2017) assessed the uncertainties in emissions inventories for China and recommended that field studies were used to improve emission estimates.

The MEIC includes emissions from five sectors: power plants, transportation, industrial, agricultural and residential sources with VOC emissions collated by functional group. As no agricultural land was present within

555   the flux footprint agricultural emissions are not considered here. Within the MEIC inventory VOCs are grouped into classes. Nine of these groupings were considered but those containing alkanes were not considered as alkanes have a proton affinity less than that of water and could not be detected using PTR-MS. The groupings, based on the speciation used by the RADM2 chemical mechanism, are summarised in Table 3.

VOC emissions estimates for the summer campaign period were calculated through combination of the flux

560   footprint (100 m x 100 m) and high resolution (3 km $\times$ 3 km) MEIC v1.3 inventory. First, the footprint for each flux aggregation period and the inventory grid for the corresponding hour of day were aligned by transforming the flux footprint into the coordinate reference system of the inventory. Subsequently the inventory values were extracted at the centre of each footprint grid cell, creating a pseudo 100 m x 100 m inventory. This was multiplied by the footprint grid, weighting each cell by their contribution to the measured flux. There was little variation

565   between VOC emission factors from the main four emissions inventory cells contributing to the flux observed at the IAP tower site. For this comparison a version of the MEIC v1.3 inventory for 2013, optimised by fitting the nested air quality prediction system (NAQPMS) model with measured pollutant concentrations during the campaign periods, was used (Du et al., 2019; Squires et al. 2020).

570

Table 3. The measured compounds used to validate the MEIC VOC groupings.

MEIC VOC grouping	Definition	Measured compounds
HCHO	Formaldehyde	formaldehyde
ALD	acetaldehyde and higher saturated aldehydes	acetaldehyde; butanal
CH3OH	Methanol	methanol
C2H5OH	Ethanol	ethanol + formic acid
TOL	toluene and less reactive aromatics	toluene; benzene
XYL	xylene and more reactive aromatics	C2 benzenes; C3 benzenes; C4 benzenes; naphthalene; C11H14
KET	Ketones	acetone; pentanone
ISO	Isoprene	isoprene
ORA2	acetic acid and higher acids	acetic acid; propionic acid

Fig. 10 shows the comparison between measured VOC emission (summer campaign) and the VOC emission predicted by the MEIC inventory for this period with the percentage contribution of each group to the total flux

575   displayed in Fig. 11. Measured emissions of aromatic compounds were 3% and 4% of those predicted by the inventory for TOL and XYL (low mass and high mass aromatics). Squires et al. (2020) compared NO_x and CO fluxes recorded during the APHH-Beijing campaigns with the MEIC inventory and also observed a similar

overestimation of emissions by the inventory for the fluxes of NO_x by a factor of 4.2 to 25 and of CO by a factor

of 1.6 to 9.7 in summer. Industrial emissions make the largest contribution to aromatic VOC emission in the

580   inventory. However, inspection of the flux footprint reveals few potential industrial sources with the footprint

encompassing roads and residential building as well as shops and restaurants. At MEIC's native 9×9 km

resolution the TOL emission peaked at 25 nmol m^{-2} s^{-1}, 9 times higher than the measured flux indicating that the

overestimate was in part caused by the proxies used to downscale the inventory to 3 km. The allocation of

industrial emissions to this residential area is likely a result of downscaling the emissions using proxies such as

585   population (Zheng et al., 2017). Even discounting the industrial emissions, the predicted emissions of TOL and

XYL are still 8 times larger than the measured flux at the 3 by 3 km resolution. The inventory does capture the

diurnal cycle in emissions with a rapid increase in aromatic VOC emissions at 07:00, emissions remaining high

throughout the day before decreasing after 17:00.

Atmospheric
Chemistry
and Physics
Discussions

Open Access

EGU
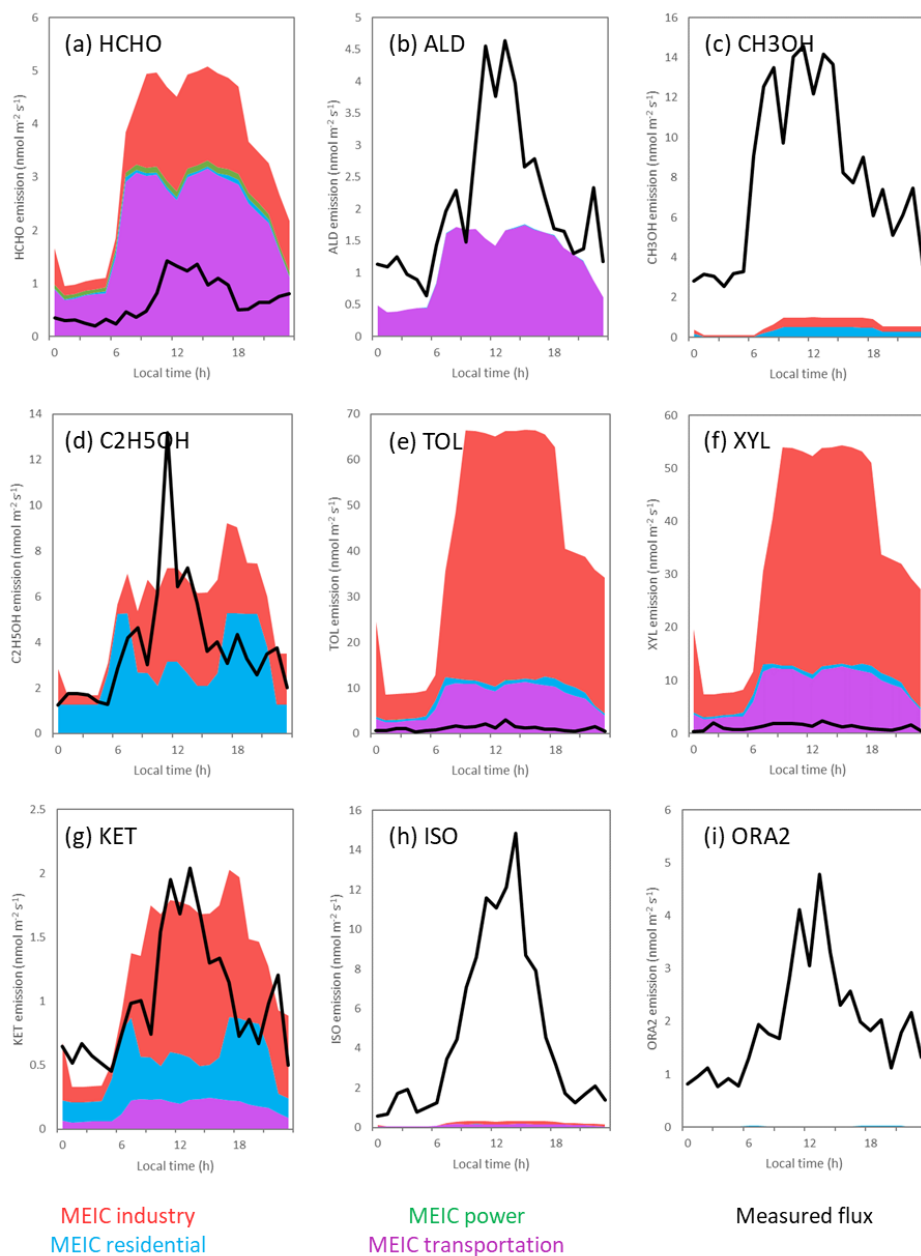
590

Figure 10. Comparison of 9 VOC classes from the MEIC emissions inventory (Table 3) with measured VOC flux (black line).
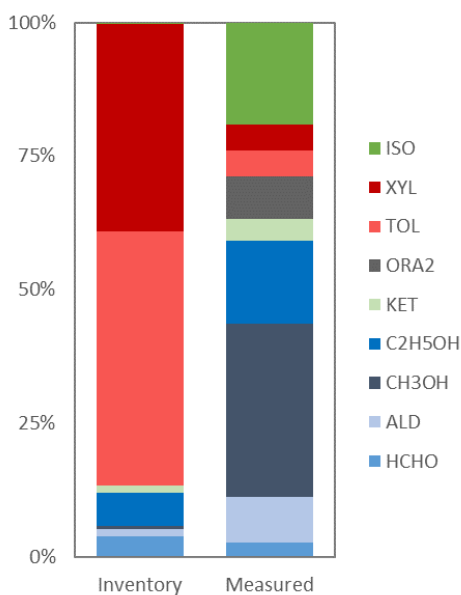
Figure 11. The percentage contribution of the MEIC VOC groupings to the total emission.

Isoprene emissions are significantly underrepresented in the inventory with measured fluxes 20 times higher than inventory emissions. This is expected as the inventory only considers anthropogenic emission and in the summer isoprene emissions are dominated by biogenic isoprene. The park at the base of the tower means that a larger biogenic source may be present at the IAP site than would on average be expected for Beijing.

The performance of the inventory in relation to oxygenated VOCs variated considerably between chemical classes. The inventory was more accurate when estimating emissions of ethanol, formaldehyde and ketones with measured emissions 71, 20 and 81% of inventory emissions. When industrial emissions are removed this increases to 132, 30 and 194% of measured emissions suggesting that ketone emission are significantly underestimated from residential and transport sources and this although the PTRMS only captured two ketones. Measured methanol, aldehydes and organic acid fluxes were also underestimated by the inventory with the measured flux 13, 1.8 and 107 times higher than the inventory, respectively.

It is likely that some underestimation of methanol, aldehydes and organic acid fluxes can be explained by their formation in the atmosphere following the oxidation of primary-emitted biogenic (e.g. Lee et al. 2006; Acton et al., 2018) or anthropogenic compounds (Atkinson, 2000). It is known that compounds such as methyl vinyl ketone and methacrolein (MVK+MACR; these compounds cannot be separated using PTR-MS) can be formed by the photo-oxidation of isoprene below the measurement height. This is supported by the high correlation between the fluxes of isoprene and MVK+MACR shown in Fig. 8. In addition to chemical sources, consumer goods are a large source of oxygenated VOCs (Dinh et al., 2015; Nematollahi et al., 2019). The use of these products is likely to vary considerably between households making bottom-up emission hard to estimate.

4 Conclusions

VOC flux measurements have been recorded for the first time over Beijing with emissions dominated by small oxygenated compounds methanol, acetaldehyde and ethanol and formic acid which could not be separated. Mixing

620   ratios of most species were significantly higher in the winter than in the summer with VOCs following the "saw tooth pattern" driven by meteorology that has been reported for other pollutants (e.g. Jia et al. 2008). Mixing ratios of aromatic compounds were lower in the summer than in the winter but mixing ratios of small oxygenated VOCs such as methanol were higher, possible as a result of increased photochemistry but also consistent with their larger emission fluxes.

625   Stagnant air masses in the winter lead to weak turbulent transport making it more difficult to determine their surface emission rate using the micrometeorological eddy covariance method. The observed VOC fluxes in the winter were weaker than those recorded in the summer probably due to low volatilisation of VOCs and deposition of VOCs transported from outside the city. The flux in both seasons was dominated by small oxygenated compounds: methanol, acetaldehyde and ethanol + formic acid. These compounds are known to be oxidation

630   products but are also present in many consumer goods products. Fluxes of aromatic compounds in the summer campaign were comparable to those observed over London and Manchester (Langford et al., 2009; Valach et al., 2016; Vaughan et al., 2017) despite the mixing ratios being larger than those observed in those cities. This suggests that the elevated mixing ratios are driven by transport from outside the city. Comparison of measured VOC fluxes with those predicted by the emissions inventory showed that the inventory failed to capture VOC emission at this

635   local scale.

Isoprene and monoterpenes, compounds predominantly emitted from biogenic sources, contributed 13% to the measured molar flux of VOCs but just 3% of the total recorded VOC mixing ratio. Comparatively, oxygenated compounds made up 60% of the molar flux of the compounds resolved by PTR-MS, aromatic compounds made up 7% and other alkenes contributed a further 11%. However, the high reactivity of isoprene and monoterpenes

640   means that their contribution to ozone and PAN formation was greater, with biogenic VOCs representing 30 and 28% of the flux contribution to ozone and PAN formation potential, respectively. This effect is even larger in respect to the OH reactivity, where biogenic VOCs represent 50% of the total potential OH reactivity of the VOCs emitted and 21% of the mixing ratio when scaled by OH reactivity. Establishing local scale activity data and improved proxies for the scaling of emissions should therefore be a priority when further developing emission

645   inventories for Beijing.

The relatively small emissions of anthropogenic VOC species from central Beijing compared to the large mixing ratios observed suggest that the scope for policy interventions focusing on VOC emission from central Beijing is limited and that the focus must therefore be on emissions controls in regions surrounding the megacity. Biogenic compounds make significant contribution to the photochemical ozone creation potential (POCP), photochemical

650   peroxyacyl nitrates (PAN) creation potential (PPCP) and potential OH reactivity emitted from the city but currently contribute only a small proportion of total reactivity in the atmosphere. However, as transport of VOCs from outside the city is reduced in the future by policy interventions, biogenic sources within the city are likely to become increasingly important to atmospheric chemistry. It is therefore important that emission inventories of VOCs in Beijing should also include an estimate of biogenic VOC emissions, using a tool such as MEGAN with

655   appropriate leaf area index and emission factor values.

Atmospheric
Chemistry
and Physics
Discussions
Open Access
EGU

Data availability. Data are available at https://catalogue.ceda.ac.uk/uuid/7ed9d8a288814b8b85433b0d3fec0300 (last access: 08/04/2020). Specific data are available from the authors on request (w.acton@lancaster.ac.uk).

660 **Author contributions**. WJFA made VOC concentration measurements, calculated VOC fluxes and performed VOC data analysis. WJFA prepared the manuscript with contributions from co-authors. ZH, ZW and BD assisted with VOC concentration measurements. FAS made NOx concentration measurements, calculated their flux and reviewed the manuscript. EN, BL and NM set up instrumentation on the twoer, measured wind vector data, provided advice on flux calculations and reviewed the manuscript. WSD, ARV and SM provided support

665 calculating fluxes using eddy4R software and reviewed manuscript. YL performed MEGAN analysis. QZ provided high resolution emissions data. MH processed the raw emissions data into gridded format for comparison with the measured fluxes. OW assisted with interpretation of the inventory emissions data and provided a detailed review of the manuscript. XW and YZ prepared the PTR-MS instrument and calibration system. PF maintained the tower and site necessary for this work. CER and JL reviewed the manuscript. CNH interpreted data, helped

670 prepare the manuscript and reviewed the manuscript.

Competing interests. The authors declare that they have no conflict of interest.

Acknowledgements

690

References

Acton W.J.F., Schallhart S., Langford B., Valach A., Rantala P., Fares S., Carriero G., Tillmann R., Tomlinson S.J., Dragosits U., Gianelle D., Hewitt C.N. and Nemitz E.: Canopy-scale flux measurements and bottom-up

695   emission estimates of volatile organic compounds from a mixed oak and hornbeam forest in northern Italy, 16(11), 7149-7170, 2016.

Acton W.J.F., Jud W., Ghirardo A., Wohlfahrt G., Hewitt C.N., Taylor J.E., Hansel A.: The effect of ozone fumigation on the above- and below-ground emissions of biogenic volatile organic compounds (BVOCs) from Brassica napus, PloS one, 1-28, 2018.

700   Atkinson R.: Atmospheric chemistry of VOCs and NOx, Atmospheric Environment, 34, 2063-2101, 2000.

Aubinet M., Vesala T., and Papale D. (Eds.): Eddy covariance: A practical guide to measurement and data analysis, Springer, Dordrecht, Heidelberg, London, New York, 438 pp., 2012.

de Gouw J.A., Warneke C., Parrish D.D., Holloway J.S., Trainer M. and Fehsenfeld F.C.: Emission sources and ocean uptake of acetonitrile (CH3CN) in the atmosphere, Journal of Geophysical Research, 108(D11), 4329,

705   2003.

Derwent R.G., Jenkin M.E., Saunders S.M. and Pilling M.J.: Photochemical ozone creation potentials for organic compounds in northwest Europe calculated with a master chemical mechanism, Atmospheric Environment, 32(14-15), 2429-2441, 1998.

Dinh T.-V., Kim S.-Y., Son Y.-S., Choi I.-Y., Park S.-R., Sunwoo Y. and Kim J.-C.: Emission characteristics of

710   VOCs emitted from consumer and commercial products and their ozone formation potential, Environmental Science and Pollution Research, 22, 9345-9355, 2015.

Du H., Li J., Chen X., Wang Z., Sun Y., Fu P., Li J., Gao J., and Wei Y.: Modeling of aerosol property evolution during winter haze episodes over a megacity cluster in northern China: roles of regional transport and heterogeneous reactions of SO2, Atmospheric Chemistry and Physics, 19, 9351–9370, 2019.

715   Dunmore R.E., Whalley L.K., Sherwen T., Evans M.J., Heard D.E., Hopkins J.R., Lee J.D., Lewis A.C., Lidster R.T., Rickard A.R. and Hamilton J.F.: Atmospheric ethanol in London and the potential impacts of future fuel formulations, Faraday Discussions, 189, 105, 120, 2016.

Ehn M., Thornton J.A., Kleist E., Sipilä M., Junninen H., Pullinen I., Springer M., Rubach F., Tillmann R., Lee B., Lopez- Hilfiker F., Andres S., Acir I.-H., Rissanen M., Jokinen T., Schobesberger S., Kangasluoma J.,

720   Kontkanen J., Nieminen T., Kurtén T., Nielsen L.B., Jørgensen S., Kjaergaard H.G., Canagaratna M., Maso M.D., Berndt T., Petäjä T., Wahner A., Kerminen V.-M., Kulmala M., Worsnop D.R., Wildt J., and Mentel T.F.: A large source of low-volatility secondary organic aerosol, Nature, 506, 476–479, 2014.

Fehsenfeld F., Calvert J., Fall R., Goldan P., Guenther A.B., Hewitt C.N., Lamb B., Liu S., Trainer M., Westberg H., and Zimmerman P.: Emissions of volatile organic compounds from vegetation and the implications for atmospheric chemistry, Global Biogeochemical Cycles, 6, 389–430, 1992.

Foken T. and Wichura B.: Tools for quality assessment of surface- based flux measurements, Agricultural and Forest Meteorology, 78, 83–105, 1996.

Gao M., Guttikunda S.K., Carmichael G.R., Wang Y., Liu Z., Stanier C.O., Saide P.E. and Yu M.: Health impacts and economic losses assessment of the 2013 severe haze event in Beijing area, Science of the Total Environment, 511, 553-561, 2015.

Ghirardo A., Xie J., Zheng X., Wang Y., Grote R., Block K., Wildt J., Mentel T., Kiendler-Scharr A., Hallquist M., Butterbach-Bahl K. and Schnitzler J.-P.: Urban stress-induced biogenic VOC emissions and SOA-forming potentials in Beijing, Atmospheric Chemistry and Physics, 16, 2901-2920, 2016.

Guenther A., Karl T., Harley P., Wiedinmyer C., Palmer P.I., Geron C.: Estimates of global terrestrial isoprene emissions using MEGAN (Model of Emissions of Gases and Aerosols from Nature), Atmospheric Chemistry and Physics, 6, 3181-3210, 2006.

Guenther A.B., Jiang X., Heald C.L., Sakulyanontvittaya T., Duhl T., Emmons L.K. and Wang X.: The model of emissions of gases and aerosols from nature version 2.1 (MEGAN2.1): An extended and updated framework for modeling biogenic emissions, Geoscientific Model Development, 5, 1471-1492, 2012.

Hallquist M., Wenger J.C., Baltensperger U., Rudich Y., Simpson D., Claeys M., Dommen J., Donahue N.M., George C., Goldstein A.H., Hamilton J.F., Herrmann H., Hoffmann T., Iinuma Y., Jang M., Jenkin M.E., Jimenez J.L., Kiendler-Scharr A., Maenhaut W., McFiggans G., Mentel Th.F., Monod A., Prévôt A.S.H., Seinfeld J.H., Surratt J.D., Szmigielski R., and Wildt J.: The formation, properties and impact of secondary organic aerosol: current and emerging issues, Atmospheric Chemistry and Physics, 9, 5155–5236, 2009.

Hartmann J., Gehrmann M., Kohnert K., Metzger S., and Sachs T.: New calibration procedures for airborne turbulence measurements and accuracy of the methane fluxes during the AirMeth campaigns, Atmospheric Measurement Techniques, 11, 4567-4581, 2018.

Holzinger R., Jordan A., Hansel A. and Lindinger W.: Automobile emissions of acetonitrile: Assessment of its contribution to the global source, Journal of Atmospheric Chemistry, 38(2), 187-193, 2001.

Hu J., Chen J., Ying Q. and Zhang H.: One-year simulation of ozone and particulate matter in China using WRF/CMAQ modeling system, Atmospheric Chemistry and Physics, 16, 10333-10350, 2016.

Jacob D.J., Field B.D., Li Q., Blake D.R., de Gouw J., Warneke C., Hansel A., Wisthaler A., Singh H.B. Guenther A.: Global budget of methanol: Constraints from atmospheric observations. Journal of Geophysical Research, 110, D08303, 2005.

755   Jia Y.T., Rahn K.A., He K.B., Wen T.X., and Wang Y.S.: A novel technique for quantifying the regional
        component of urban aerosol solely from its sawtooth cycles, Journal of Geophysical Research-Atmospheres,
        113, D21309, 2008.

        Jordan A., Haidacher S., Hanel G., Hartungen E., Märk L., Seehauser H., Schottkowsky R., Sulzer P. and Märk
        T.D.: A high resolution and high sensitivity proton-transfer-reaction time-of-flight mass spectrometer (PTR-
760   TOF-MS), 286(2-3), 122-128, 2009.

        Karl T.G., Spirig C., Rinne J., Stroud C., Prevost P., Greenberg J., Fall R., and Guenther A.: Virtual disjunct
        eddy covariance measurements of organic compound fluxes from a subalpine forest using proton transfer
        reaction mass spectrometry, Atmospheric Chemistry and Physics, 2, 279–291, 2002.

        Karl T., Jobson T., Kuster W.C., Williams E., Stutz J., Shetter R., Hall S.R., Goldan P. and Fehsenfeld F.: Use
765   of proton-transfer-reaction mass spectrometry to characterize volatile organic compound sources at the La Porte
        super site during the Texas Air Quality Study 2000, Journal of Geophysical Research, 108(D16), 4508, 2003.

        Kljun N., Calanca P., Rotach M.W., and Schmid H.P.: A simple parameterisation for flux footprint predictions,
        Boundary-Layer Meteorology, 112, 503–523, 2004.

        Lee A., Goldstein A.H., Keywood M.D., Gao S., Varutbangkul V., Bahreini R., Ng N.L., Flagan R.C. and
770   Seinfeld J.H.: Gas-phase products and secondary aerosol yields from the ozonolysis of ten different terpenes,
        Journal of Geophysical Research Atmospheres, 111(7), 1-18, 2007.

        Lindinger, WernerKarl T., Striednig M., Graus M., Hammerle A., Wohlfahrt G.: Urban flux measurements
        reveal a large pool of oxygenated volatile organic compound emissions, PNAS, 2018.
        https://doi.org/10.1073/pnas.1714715115

775   Langford B., Davison B., Nemitz E. and Hewitt C.N.: Mixing ratios and eddy covariance flux measurements of
        volatile organic compounds from an urban canopy (Manchester, UK), Atmospheric Chemistry and Physics, 9,
        1971-1987, 2009.

        Langford B., Misztal P. K., Nemitz E., Davison B., Helfter C., Pugh T. A. M., MacKenzie A. R., Lim S. F., and
        Hewitt C. N.: Fluxes and concentrations of volatile organic compounds from a South-East Asian tropical
780   rainforest, Atmospheric Chemistry and Physics, 10, 8391–8412, 2010.

        Langford B., Nemitz E., House E., Phillips G.J., Famulari D., Davison B., Hopkins J.R., Lewis A.C. and Hewitt
        C.N.: Fluxes and concentrations of volatile organic compounds above central London, UK, Atmospheric
        Chemistry and Physics, 10, 627–645, 2010.

        Langford B., Acton W., Ammann C., Valach A., and Nemitz E.: Eddy-covariance data with low signal-to-noise
785   ratio: time-lag determination, uncertainties and limit of detection, Atmospheric Measurement Techniques, 8,
        4197–4213, 2015.

        Langford B., Cash J., Acton W.J.F., Valach A.C., Hewitt C.N., Fares S., Goded I., Gruening C., House E.,
        Kalogridis A.-C., Gros V., Schafers R., Thomas R., Broadmeadow M. and Nemitz E.: Isoprene emission

potentials from European oak forests derived from canopy flux measurements: An assessment of uncertainties
790 and inter-algorithm variability, Biogeosciences, 14, 5571-5594, 2017.

Lenschow D.H., Mann J. and Kristensen L.: How long is long enough when measuring fluxes and other
turbulence statistics, Journal of Atmospheric and Ocean Technology, 11, 661-673, 1994.

Li K., Li J., Wang W., Tong S., Liggio J. and Ge M.: Evaluating the effectiveness of joint emission control
policies on the reduction of ambient VOCs: Implications from observation during the 2014 APEC summit in
795 suburban Beijing, Atmospheric Environment, 164, 117-127, 2017.

Liu Y., Yuan B., Li X., Shao M., Lu S., Li Y., Chang C.C., Wang Z., Hu W., Huang X., He L., Zeng L., Hu M.
and Zhu T.: Impact of pollution controls in Beijing on atmospheric oxygenated volatile organic compounds
(OVOCs) during the 2008 Olympic Games: Observation and modeling implications, Atmospheric Chemistry
and Physics, 15, 3045-3062, 2015.

800 Metzger S., Junkermann W., Mauder M., Beyrich F., Butterbach-Bahl K., Schmid H.P., and Foken, T.: Eddy-
covariance flux measurements with a weight-shift microlight aircraft, Atmospheric Measurement Techniques, 5,
1699–1717, 2012.

Metzger S., Durden D., Sturtevant C., Luo H., Pingintha-Durden N., Sachs T., Serafimovich A., Hartmann J., Li
J.H., Xu K., and Desai A.R.: eddy4R 0.2.0: a DevOps model for community-extensible processing and analysis
805 of eddy-covariance data based on R, Git, Docker, and HDF5, Geoscientific Model Development, 10, 3189–
3206, 2017.

Müller M., Graus M., Ruuskanen T.M., Schnitzhofer R., Bamberger I., Kaser L., Titzmann T., Hörtnagl L.,
Wohlfahrt G., Karl T. and Hansel A.: First eddy covariance flux measurements by PTR-TOF, Atmospheric
Measurement Techniques, 3, 387-395, 2010.

810 Müller M., Mikoviny T., Jud W., D'Anna B. and Wisthaler A.: A new software tool for the analysis of high
resolution PTR-TOF mass spectra, 127, 158-165, 2013.

Nematollahi N., Kolev S.D. and Steinemann A.: Volatile chemical emissions from 134 common consumer
products, Air Quality, Atmosphere & Health, https://doi.org/10.1007/s11869-019-00754-0, 2019.

Qi J., Zheng B., Li M., Yu F., Chen C., Liu F., Zhou X., Yuan J., Zhang Q., and He K.: A high-resolution air
815 pollutants emission inventory in 2013 for the Beijing-Tianjin-Hebei region, China, Atmospheric Environment,
170, 156–168, 2017.

Ren Y., Qu Z., Du Y., Xu R., Ma D., Yang G., Shi Y., Fan X., Tani A., Guo P., Ge Y. and Chang J.: Air quality
and health effects of biogenic volatile organic compounds emissions from urban green spaces and the mitigation
strategies, Environmental Pollution, 230, 849-861, 2017.

820 Shao M., Lu S., Liu Y., Xie X., Chang C., Huang S. and Chen Z.: Volatile organic compounds measured in
summer in Beijing and their role in ground-level ozone formation, Journal of Geophysical Research
Atmospheres, 114(D00G06), 1-13, 2009.

Atmospheric
Chemistry
and Physics
Discussions

Shi Z., Vu T., Kotthaus S., Harrison R.M., Grimmond S., Yue S., Zhu T., Lee J., Han Y., Demuzere M.,
Dunmore R.E., Ren L., Liu D., Wang Y., Wild O., Allan J., Acton W.J., Barlow J., Barratt B., Beddows D.,

825   Bloss W.J., Calzolai G., Carruthers D., Carslaw D.C., Chan Q., Chatzidiakou L., Chen Y., Crilley L., Coe H.,
Dai T., Doherty R., Duan F., Fu P., Ge B., Ge M., Guan D., Hamilton J.F., He K., Heal M., Heard D., Hewitt
C.N., Hollaway M., Hu M., Ji D., Jiang X., Jones R., Kalberer M., Kelly F.J., Kramer L., Langford B., Lin C.,
Lewis A.C., Li J., Li W., Liu H., Liu J., Loh M., Lu K., Lucarelli F., Mann G., Mcfiggans G., Miller M.R., Mills
G., Monk P., Nemitz E., Ouyang B., Palmer P.I., Percival C., Popoola O., Reeves C., Rickard A.R., Shao L., Shi

830   G., Spracklen D., Stevenson D., Sun Y., Sun Z., Tao S., Tong S., Wang Q., Wang W., Wang X., Wang X.,
Wang Z., Wei L., Whalley L., Wu X., Wu Z., Xie P., Yang F., Zhang Q., Zhang Y., Zhang Y., and Zheng M.:
Introduction to the special issue " In-depth study of air pollution sources and processes within Beijing and its
surrounding region (APHH-Beijing)", Atmospheric Chemistry and Physics, 19, 7519-7546, 2019.

Spirig C., Neftel A., Ammann C., Dommen J., Grabmer W., Thielmann A., Schaub A., Beauchamp J., Wisthaler

835   A., and Hansel A.: Eddy covariance flux measurements of bio- genic VOCs during ECHO 2003 using proton
transfer re- action mass spectrometry, Atmospheric Chemistry and Physics, 5, 465–481, 2005.

Squires F.A., Nemitz E., Langford B., Wild O., Drysdale W.S., Acton W.J.F., Fu P., Grimmond C.S.B.,
Hamilton J.F., Hewitt C.N., Hollaway M., Kotthaus S., Lee J., Metzger S., Pingintha-Durden N., Shaw M.,
Vaughan A.R., Wang X., Wu R., Zhang Q. and Zhang Y.: Measurements of traffic dominated pollutant

840   emissions in a Chinese megacity. Atmospheric Chemistry and Physics Discussions, https://doi.org/10.5194/acp-
2019-1105, 2020.

Steinemann A.: Volatile emissions from common consumer products, Air Quality, Atmosphere & Health, 8,
273-281, 2015.

Taipale R., Ruuskanen T.M., Rinne J., Kajos M.K., Hakola H., Pohja T. and Kulmala M.: Technical Note:

845   Quantitative long-term measurements of VOC concentrations by PTR-MS – measurement, calibration, and
volume mixing ratio calculation methods, Atmospheric Chemistry and Physics, 8, 9435-9475, 2008.

Taipale R., Ruuskanen T.M., and Rinne J.: Lag time determination in DEC measurements with PTR-MS,
Atmospheric Measurement Techniques, 3, 853–862, 2010.

Tani A., Hayward S., Hansel A. and Hewitt C.N.: Effect of water vapour pressure on monoterpene

850   measurements using pro- ton transfer reaction-mass spectrometry (PTR-MS), International Journal of Mass
Spectrometry, 239, 161–169, 2004.

Valach A.C., Langford B., Nemitz E., Mackenzie A.R. and Hewitt C.N.: Seasonal and diurnal trends in
concentrations and fluxes of volatile organic compounds in central London, Atmospheric Chemistry and
Physics, 15, 7777-7796, 2015.

855   Vaughan A.R., Lee J.D., Shaw M.D., Misztal P.K., Metzger S., Vieno M., Davison B., Karl T.G., Carpenter
L.J., Lewis A.C., Purvis R.M., Goldstein A.H. and Hewitt C.N.: VOC emission rates over London and South
East England obtained by airborne eddy covariance, Faraday Discussions, 200, 599–620, 2017.

Wang M., Shao M., Chen W., Lu S., Liu Y., Yuan B., Zhang Q., Zhang Q., Chang C.C., Wang B., Zeng L., Hu
M., Yang Y. and Li Y.: Trends of non-methane hydrocarbons (NMHC) emissions in Beijing during 2002-2013,
860   Atmospheric Chemistry and Physics, 15, 1489-1502, 2015.

Wehner B., Birmili W., Ditas F., Wu Z., Hu M., Liu X., Mao J., Sugimoto N. and Wiedensohler A.:
Relationships between submicrometer particulate air pollution and air mass history in Beijing, China, 2004-
2006, Atmospheric Chemistry and Physics, 8, 6155–6168, 2008.

Yang Z., Wang H., Shao Z., and Muncrief R.: Review of Beijing's Comprehensive Motor Vehicle Emission
865   Control Programs, International Council on Clean Transportation Europe, Berlin, 2015.

Yuan B., Shao M., de Gouw J., Parrish D.D., Lu S., Wang M., Zeng L., Zhang Q., Song Y., Zhang, J. and Hu
M.: Volatile organic compounds (VOCs) in urban air: How chemistry affects the interpretation of positive
matrix factorization (PMF) analysis, Journal of Geophysical Research Atmospheres, 117(D24302),1-17, 2012.

Zhang, H.N., Zhang, Y.L., Huang, Z.H., Wang, Z.Y., Acton, W., Nemitz, E., Langford, B., Mullinger, N.,
870   Davison, B., Shi, Z.B., Liu, D., Yang, W.Q., Zeng, J.Q., Wu, Z.F., Fu, P.Q., Zhang, Q., Wang, X.M.: Vertical
profiles of BVOCs observed by proton transfer reaction-time of flight-mass spectrometry at the 325-meter IAP
tower in Beijing. Journal of Environmental Science (2019), Accepted.

Zhang L., Wang T., Lv M. and Zhang Q.: On the severe haze in Beijing during January 2013: Unraveling the
effects of meteorological anomalies with WRF-Chem, Atmospheric Environment, 104, 11-21, 2015.

875   Zhao Y., Zhou Y.D., Qiu L.P. and Zhang J.: Quantifying the uncertainties of China's emission inventory for
industrial sources: From national to provincial and city scales, Atmospheric Environment, 165, 207–221, 2017.

Zheng B., Zhang Q., Tong D., Chen C., Hong C., Li M., Geng G., Lei Y., Huo H. and He K.: Resolution
dependence of uncertainties in gridded emission inventories: a case study in Hebei, China, Atmospheric
Chemistry and Physics, 17, 921-933, 2017.